



INSTITUTO SUPERIOR TÉCNICO
Universidade Técnica de Lisboa



Jactos pulsados laminares

Características propulsivas

Rui Vizinho de Oliveira

Dissertação para obtenção do Grau de Mestre em

Engenharia Aeroespacial

(Resumo Alargado)

Júri

Presidente: Professor Fernando José Parracho Lau

Orientador: Professor João Manuel Melo de Sousa

Vogais: Professor Carlos Frederico Neves Bettencourt da Silva

Outubro de 2010

Summary:

The validation process of the numerical analysis demonstrated the capability of the numerical model and designed mesh to provide us with results in good agreement with theory and experimental data. A general numerical study of the formation process of vortex rings was made in order to understand its dynamics and to confirm earlier observed behaviors during this phase. The main purpose of the present paper is to establish a comparison between pulsed jets and constant ones, in order to determine which one is more efficient in terms of energy, momentum or mass. In the process of this evaluation, different velocity programs and ejector geometries are studied so as to acknowledge the influence of each feature in the propulsive gain of the pulsed jet versus the constant jet mode. A brief hypothesis on squid locomotion behavior is proposed.

Introduction:

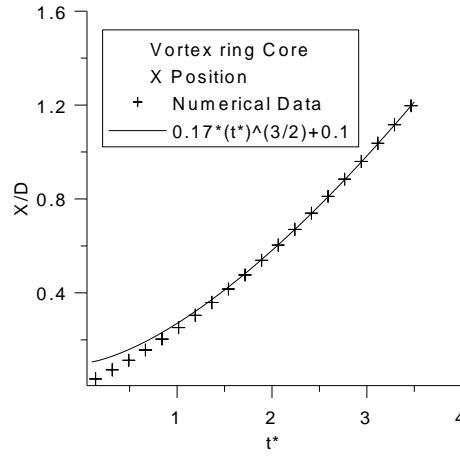
Vortex rings have been registered and studied by Didden [2] using a piston mechanism with a nozzle ejector, where the location of the vortex core was acquired using an injected dye. The resulting data was compared to the similarity theory modeled by Saffman [7] and Pullin [6]. Other studies were done over the vortex ring formation phase by Gharib, Rambod and Shariff [3], where they concluded that it appeared to exist a universal non-dimensional scale limiting the vortex formation process, the formation number, defined in equation (1).

$$\frac{L}{D} = \frac{\int_0^{t_{ejec}} U_{cf}(t) dt}{D} \quad (1)$$

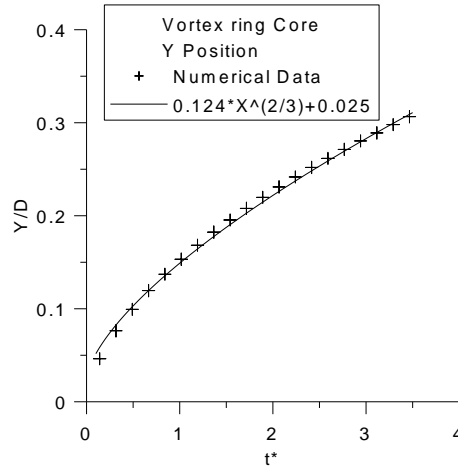
Typical values found for this scale were 3.6~4.5. In the work of Dabiri [1], it is observed that some biological systems that produce vortex rings tend to maximize these fluid structures by reaching the formation number limit mentioned earlier, thus providing us with the hint that vortex ring based propulsion might be more efficient than a constant jet mode. Krueger *et al.* [5] built a mechanical, self-propelled, pulsed-jet vehicle (Robosquid) to use under water. They concluded that thrust augmentation was achieved by using a pulsed jet mode, and that the apparent additional energy required to operate the vehicle was low compared to the impulse benefit of the pulsed jet, though no data referring to energy consumption is presented in their paper.

Validation:

The validation process performed was divided in two stages. The stationary validation where a constant laminar jet was analyzed and its properties were compared with theoretical predictions, which were in good agreement. The second stage of validation focused on the unsteady flow of a pulsed jet, where the formation process of the vortex ring was analyzed and compared with theory and experimental data, again resulting in good agreement. For the validation runs, the dimensionless time increment selected was 0.0175 based on a convergence study and the orifice exit diameter was 4 mm. In all numerical runs the maximum velocity imposed at the velocity-inlet boundary was 7 m/s, implying that a maximum Reynolds number of about 2000 is reached during every simulation performed on the present work. Hence, only laminar flows were studied.



• Fig. 1 Vortex ring core axial displacement.



• Fig. 2 Vortex ring core radial displacement.

Figures 1 and 2 show the x and y coordinate positions of the vortex ring core during its initial stages of formation. As can be seen, the rate of radial growth agrees with theory as were earlier experimental data, though, axial displacement of the vortex core does not comply with it. It should be noted that this phenomenon is also observed in every experimental work done to date, therefore it can be stated that axial data obtained is in good agreement with experimental data. The reason why axial displacement is not in accordance with theory has been worked out by Yao, Jian-ping and Xungang [8]. The origin of this misbehavior is in the ring's curvature influence on it-self, making its displacement in the axial direction faster than similarity theory predicts.

Discussion:

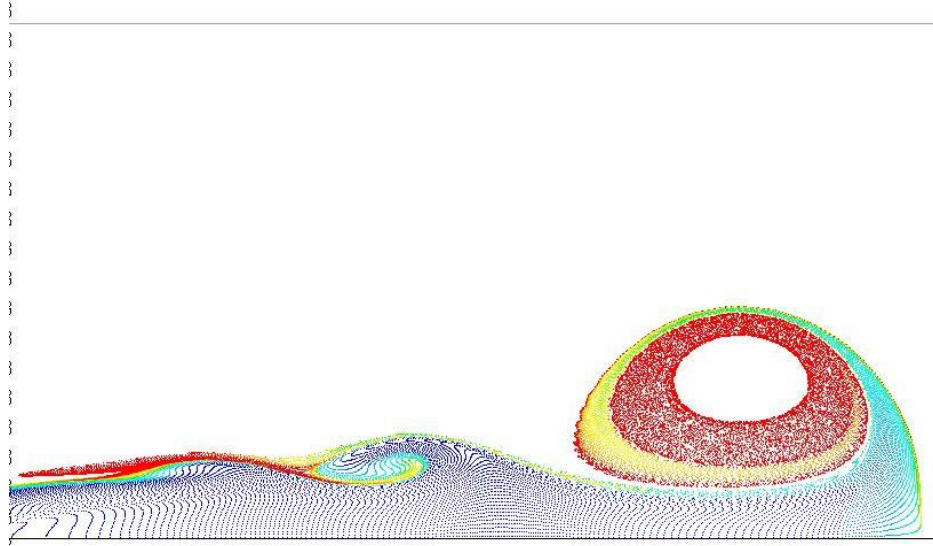
Initial phase of vortex ring formation:

In order to fully understand the process of formation of a vortex ring, the initial stages of its development were observed where it was concluded, as before, that the initial phase of the ring is a recirculation bubble that results from flow separation near the lip of the orifice through which the fluid is accelerated. After this initial stage, the bubble separates from the wall and forms a ring, the vortex ring.

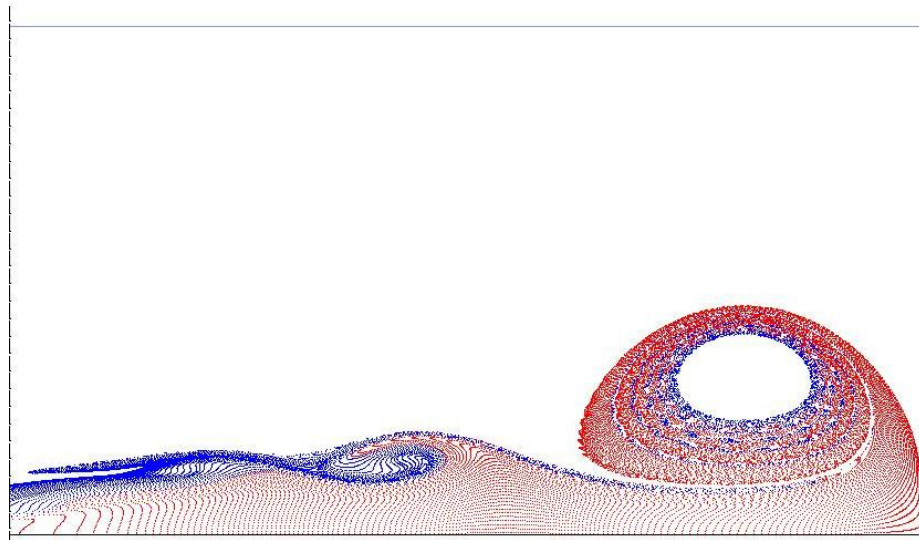
Vortex ring growth:

After the formation's initial phase, the ring will continue to grow in size and strength as long as the shear layer being ejected by the orifice is in reach. This growth process of the ring is limited,

since the ring is a self-propelled fluid structure due to its curvature. As soon as the ring reaches a certain circulation intensity, the velocity field it imposes around itself will manifest in its departure away from range of vortical shear layer ejected by the nozzle, thus ending the formation process. This phase is referred to as “pinch-off”, and it defines the formation number described above on the “Introduction” section.



- *Fig. 3 Temporal particle analysis of a long pulse jet.*

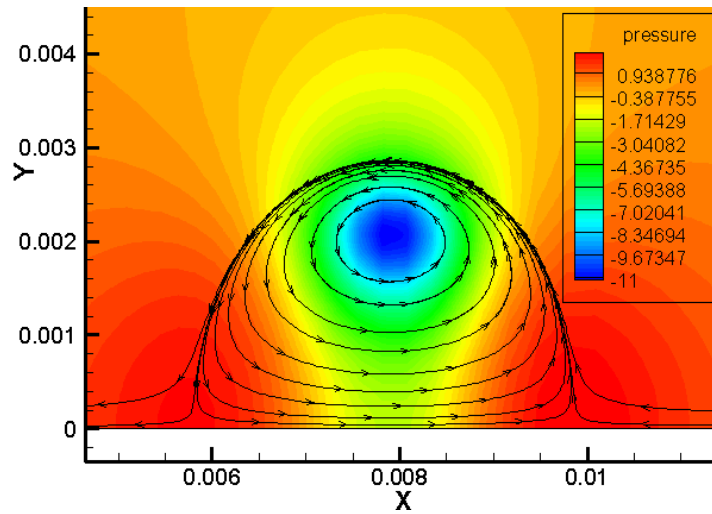


- *Fig. 4 Zone emission particle analysis of a long pulse jet.*

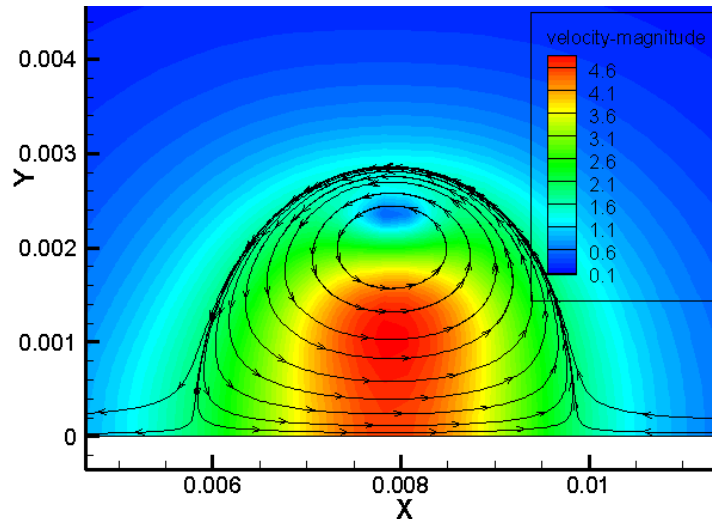
The red zones in figure 3 represent fluid that was ejected up until the formation number reached 4.5, where as in figure 4 the blue zones represent approximately the shear layer being ejected by the orifice exit. As shown, the vortex ring only entangles the shear layer ejected up to the point when the formation number reaches 4.5, when the rest of the shear layer stops being incorporated into the vortex core, ending the growth phase of the ring. The shear layer ejected in excess is concentrated in secondary vortex rings that form in the main vortex ring wake.

Pulsed Jet Static Pressure Impulse:

It is stated that the origin of the propulsive benefit from using a pulsed jet is the additional mass accelerated during vortex ring formation. Another point of view over this matter can be made by observing that centrifugal forces must be compensated by radial pressure gradients. During the vortex ring formation, its propagation through the ambient fluid induces curved streamlines, thus a centrifugal force is created and a raise in static pressure must be present in order to balance this fluid flow feature. This static pressure gradient comes from within the vortex core where static pressure drops. As we reach the outer region of the vortex ring near the ejector's wall we can see that there exists an overpressure zone.



• Fig. 5 Static Pressure and streamline map (Pa).



• Fig. 6 Velocity magnitude and streamline map (m/s).

As can be observed in the figures 5 and 6, the relation between the streamlines, the velocity magnitude and the static pressure map is self-evident. The zones of high static pressure are dominated by high streamline curvature and velocity magnitude. These maps were obtained in a reference frame moving with the vortex ring.

The calculated relative contribution of the static pressure impulse to the total impulse by the vortex ring is about 40%. This value was also found in the studies of Krueger [4] as stated in page 61 of his thesis.

Efficiency theory analysis:

In order to evaluate the efficiency of the pulsed jet versus the constant jet mode, a parameter must be chosen to be used as a comparison standard. The three parameters considered here are ejected mass, momentum impulse and kinetic energy.

In order to apply a model to the present study based on the jet characteristics, the imposed boundary values, constant for constant jet and mean values for the pulsed case were used to calculate the three parameters mentioned above. Based on these values and assuming a pure impulsive velocity program for the pulsed jet, a radial constant velocity profile and an ejector with cylinder geometry, the expressions (2)-(4) were deducted to achieve the equivalency between the two modes of operation for the jet.

$$U_{cte_{eq\ m}} = U_{max} \frac{t_{e_{jec}}}{t_{pulse}} \quad (2)$$

$$U_{cte_{eq\ M}} = U_{max} \sqrt{\frac{t_{e_{jec}}}{t_{pulse}}} \quad (3)$$

$$U_{cte_{eq\ E}} = U_{max} \sqrt[3]{\frac{t_{e_{jec}}}{t_{pulse}}} \quad (4)$$

As can be observed, the constant operation mode will always deliver a jet with a lower velocity than a pulsed one. Using these velocity equivalencies, the relation between kinetic energies applied to the fluid by the constant jet and the pulsed mode were derived and are presented in the expressions (5)-(7).

$$\frac{E_{pulsed}}{E_{cte_{eq\ m}}} = \left(\frac{t_{pulse}}{t_{e_{jec}}} \right)^2 \quad (5)$$

$$\frac{E_{pulsed}}{E_{cte_{eq\ M}}} = \sqrt{\frac{t_{pulse}}{t_{e_{jec}}}} \quad (6)$$

$$\frac{E_{pulsed}}{E_{cte_{eq\ E}}} = 1 \quad (7)$$

$$t_{pulse} > t_{e_{jec}} \Rightarrow E_{pulsed} > E_{cte_{eq\ M}} > E_{cte_{eq\ m}} \quad (8)$$

From (8), it is self-evident that for the case of pulsed jets ejecting the same mass as constant ones, the thrust will be greater. Since pulsed jets need to expel the same mass at a higher rate,

the energy applied in the process is consequently larger, thus yielding the increase in thrust versus the constant jet.

Based on these facts it is advised to use the kinetic energy parameter as a comparison standard between jet modes of operation.

Manipulation of propulsive gains:

Vortex ring formation is fairly sensitive to the velocity program applied in the ejected fluid as is to the geometry design of its ejector. In order to determine their influence, the subsequent tables represent the thrust gains of the pulsed jet versus constant jets that eject the same mass, have the same momentum impulse or use the same kinetic energy in the same pulse time.

For a typical NIVP¹ velocity program with a pulse time of $6,00857 \times 10^{-3}$ (s), the results obtained are presented in table 1.

Characteristics	Pulsed Jet	Constant Jet Mass Equivalence	Constant Jet Momentum Impulse Equivalence	Constant Jet Energy Equivalence
Mass (kg)	$2,7591 \times 10^{-7}$	$2,7591 \times 10^{-7}$	$4,2213 \times 10^{-7}$	$4,8775 \times 10^{-7}$
Momentum Impulse (N.s)	$1,9265 \times 10^{-6}$	$8,2009 \times 10^{-7}$	$1,9196 \times 10^{-6}$	$2,5627 \times 10^{-6}$
Energy (J)	$6,7814 \times 10^{-6}$	$1,2185 \times 10^{-6}$	$4,3623 \times 10^{-6}$	$6,7289 \times 10^{-6}$
Average Thrust (N)	$3,0281 \times 10^{-4}$	$1,5415 \times 10^{-4}$	$3,5547 \times 10^{-4}$	$4,7259 \times 10^{-4}$
Thrust Gain % pulsed jet vs. constant jet	-	96,4	-14,8	-35,9

• *Tab. 1 Near Impulsive velocity program results.*

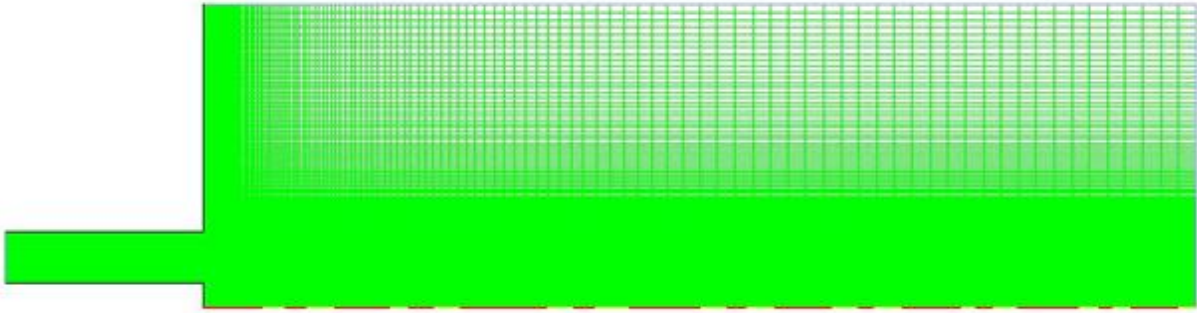
Using a parabolic ramped velocity program with a pulse time of $0,022564$ (s), the results achieved are shown in table 2.

Characteristics	Pulsed Jet	Constant Jet Mass Equivalence	Constant Jet Momentum Impulse Equivalence	Constant Jet Energy Equivalence
Mass (kg)	$4,3266 \times 10^{-7}$	$4,3264 \times 10^{-7}$	$7,8903 \times 10^{-7}$	$1,0247 \times 10^{-6}$
Momentum Impulse (N.s)	$1,8170 \times 10^{-6}$	$5,4439 \times 10^{-7}$	$1,8106 \times 10^{-6}$	$3,0540 \times 10^{-6}$
Energy (J)	$4,5838 \times 10^{-6}$	$3,4354 \times 10^{-7}$	$2,0785 \times 10^{-6}$	$4,5499 \times 10^{-6}$
Average Thrust (N)	$8,2317 \times 10^{-5}$	$2,8529 \times 10^{-5}$	$9,2756 \times 10^{-5}$	$1,5501 \times 10^{-4}$
Thrust Gain % pulsed jet vs. constant jet	-	188,5	-11,3	-46,9

• *Tab. 2 Parabolic ramped velocity program results.*

Testing the same NIVP velocity program and a different geometry for the ejector, shown in figure 7, in the particular case an annular ejector, the velocity field demonstrated the creation of a set of two vortex rings, an inner vortex ring and a larger outer vortex ring.

¹ NIVP stands for "Near Impulsive Velocity Program".



• Fig. 7 Annular ejector mesh.

Characteristics	Pulsed Jet	Constant Jet Mass Equivalence	Constant Jet Momentum Impulse Equivalence	Constant Jet Energy Equivalence
Mass (kg)	$5,5182 \times 10^{-7}$	$5,5182 \times 10^{-7}$	$9,3887 \times 10^{-7}$	$1,1247 \times 10^{-6}$
Momentum Impulse (N.s)	$3,8487 \times 10^{-6}$	$1,3261 \times 10^{-6}$	$3,8388 \times 10^{-6}$	$5,5093 \times 10^{-6}$
Energy (J)	$1,3562 \times 10^{-5}$	$1,5939 \times 10^{-6}$	$7,8837 \times 10^{-6}$	$1,3547 \times 10^{-5}$
Average Thrust (N)	$4,7310 \times 10^{-4}$	$1,9665 \times 10^{-4}$	$5,6064 \times 10^{-4}$	$8,0131 \times 10^{-4}$
Thrust Gain % pulsed jet vs. constant jet	-	140,6	-15,6	-40,9

• Tab. 3 Annular ejector results.

As can be observed, the results of table 3 show a benefit from using an annular ejector, resulting in a possible 141 % thrust gain of the pulsed jet versus the mass equivalent constant jet mode.

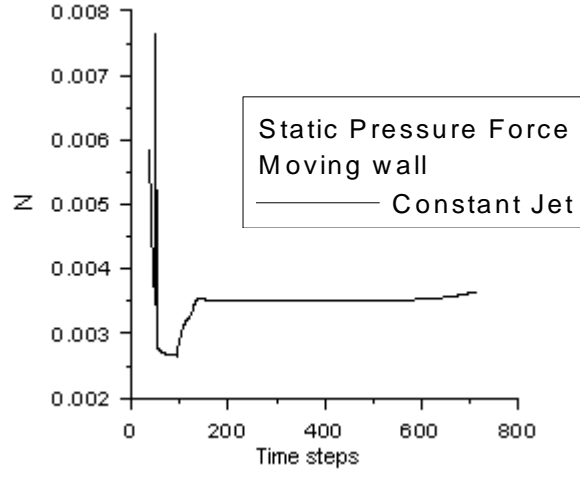
One can state that, no matter what is used to influence the propulsive gains of a pulsed jet, the latter will never have thrust augmentation versus a constant jet that uses the same kinetic energy.

Mechanical energy consumption:

Numerical analysis:

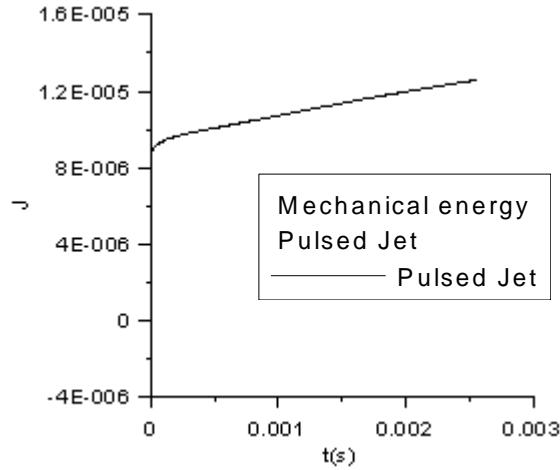
By making use of a moving mesh, it is possible to acquire the mechanical energy applied to the flow by a piston. In order to achieve this, the pressure force applied to the head of the piston is registered as its velocity during the ejection phase. At the end of the pulse, by multiplying these two values and integrating over time one acquires the mechanical energy used to produce a vortex ring.

In order to simulate a constant jet using the finite geometry of a moving mesh piston, a reservoir of fluid was designed, having a larger radius than its ejector. The purpose of such a measure was to reduce the displacement the piston had to make so as to be capable of delivering a constant jet flow with the required velocity for a long period of time. The constant jet obtained ejected the same mass in a pulse time as the pulsed jet. Based on the same principles for the pulsed case, the mechanical energy used to maintain the constant jet was obtained, though the values of pressure on the piston head used were the stable phase ones, where the jet is still constant and pressure values on the piston head have stabilized as shown in figure 8.



• Fig. 8 Pressure force on moving wall.

Knowing that in the constant jet mode the piston was moving at the speed of 0.12 (m/s), the stable pressure force on the piston head was 0.003496 (N) and that the pulse time was 5.9962×10^{-3} (s), the mechanical energy used was 2.5155×10^{-6} (J). In the pulsed case the mechanical energy calculated was 1.2584×10^{-5} (J) represented in figure 9. Both jets ejected approximately 2.7702×10^{-7} (kg) of mass, and the calculated average thrust values were 3.0919×10^{-4} (N) and 1.677×10^{-4} (N) for the pulsed and constant cases respectively.



• Fig. 9 Mechanical energy used by pulsed jet.

Though the pulsed jet has 85.5% propulsive gain over the constant jet mode, its operation requires over 400% more mechanical energy than the latter.

Biological hypothesis:

As stated on some of the articles in the literature, various biological mechanisms that use pulsed jets to operate, tend to maximize the impulse obtained from the ejected fluid pulse. This trend has its origins not on energy efficiency, but rather on the anatomic limitations of these biological systems. The purpose of optimization led by these mechanisms is to maximize the impulse obtainable with the finite amount of mass fluid that they are able to handle. Citing from Dabiri [1] article on page 26, quote:

"Whereas the transition from maximum efficiency to maximal impulse occurs as a disease pathology in the left heart, this transition occurs in squid as part of ontogenetic development from hatchling to adult, concomitant with lateral fin development."

This evolution on the propulsion means of squids might be related with the fact that, for hatchlings, the maximum formation number they are able to reach is small, meaning that they can only handle small mass amounts of water relative to their nozzle diameter, and because they are small sized, the energetic cost of locomotion is also small, thus, energetic efficient propulsion is not a primary concern to their survival. They are driven to maximize the impulse possible to obtain from the little mass of water they are capable of ejecting.

When squid reach adulthood, the maximum formation number they can reach is far greater than hatchlings, though locomotion costs are considerably higher due to their size, so squid usually use fins to move around and only resort to pulsed jets of water when threaten as a way to flee. During the squid escape, the latter attempts to maximize the impulse able to deliver by resorting to the maximization of the vortex ring formed during the initial phase of the pulsed water jet ejection. By doing this, the squid will gain higher rates of acceleration being able to swiftly escape from an immediate threat, justifying the extra energy used to optimize the pulse ejection.

After the escape's initial phase is over, the squid will continue to thrust away resorting to a more efficient constant jet mode, faster than its fins and less consuming than its pulsed jet capability. If a squid managed its water reserve so as to only eject multiple pulsed jets during an escape they would in fact reach higher rates of acceleration and speed, though, since we are dealing with a biological organism that needs to survive through multiple escape attempts, this locomotion mode would deplete its energy reserves quickly, exposing the squid to a vulnerable situation.

Conclusions:

Throughout this study the following conclusions were drawn:

- Vortex ring growth phase occurs as long as the ejected vortical shear layer is in range, the excess of ejected shear layer will form secondary vortex rings in the main vortex ring wake.
- The over-pressure applied by the vortex ring is due to streamline curvature around it and the velocity magnitude the ring's circulation imposes on the flow. In order to balance the centrifugal forces originated by this fluid structure, a gradient in static pressure must exist, where raising pressure occurs as streamline curvature and velocity magnitude increase.
- The usage of a parabolic acceleration ramp velocity program in a pulsed jet delivers a gain of 188% on average thrust versus a constant jet that uses the same mass for the same pulse time.
- The use of an annular geometry for the ejector provides us with a gain of 141% on average thrust versus a constant jet that ejects the same mass in the pulse time.
- From the use of the energy comparison parameter, it is concluded that there is no benefit on using a pulsed jet versus the constant jet mode.
- The mechanical energy consumed by the pulsed jet is about 400% higher than the mass equivalent constant jet. Conversely, the pulsed jet has a thrust increase of only about 85%. It is not energetically efficient to resort on conventional pulsed jets for propulsive means.

Bibliography

- [1] Dabiri, J. 2009. Optimal Vortex Formation as a Unifying Principle in Biological Propulsion. Annual Review of Fluid Mechanics. **Vol.41**, 17-33.
- [2] Didden, N. 1979. On the Formation of Vortex Rings Rolling-up and Production of Circulation. Journal of Applied Mathematics and Physics (ZAMP). **Vol.30**, 101-116.
- [3] Gharib, M., Rambod, E. and Shariff, K. 1998. A universal time scale for vortex ring formation. Journal of Fluid Mechanics. **Vol.360**, 121-140.
- [4] Krueger, P. 2001. Ph.D. thesis. California Institute of Technology. Pasadena, California.
- [5] Krueger, P., Moslemi, A., Nichols, J., Bartol, I. and Stewart, W. 2008. Vortex Rings in Bio-inspired and Biological Jet Propulsion. Advances in Science and Technology. **Vol.58**, 237-246.
- [6] Pullin, D. 1979. Vortex Ring Formation at Tube and Orifice Openings. Physics of Fluids. **Vol.22**, 401-403.
- [7] Saffman, P. 1978. The Number of Waves on Unstable Vortex Rings. Journal of Fluid Mechanics. **Vol.84**, 625-639.
- [8] Yao, Z., Jian-ping, W. and Xungang, S. 1998. On the formation of vortex rings and pairs. ACTA MECHANICA SINICA. **Vol.14**, **No.2**, 113-129.